# Scanning Force Microscopy at the Air-Water Interface of an Air Bubble Coated with Pulmonary Surfactant

D. Knebel,* M. Sieber,* R. Reichelt,† H.-J. Galla,* and M. Amrein†
*Institut für Biochemie and †Institut für Medizinische Physik und Biophysik, Westfälische Wilhelms-Universität, D-48149 Münster, Germany

ABSTRACT To study the structure-function relationship of pulmonary surfactant under conditions close to nature, molecular films of a model system consisting of dipalmitoylphosphatidylcholine, dipalmitoylphosphatidylglycerol, and surfactant-associated protein C were prepared at the air-water interface of air bubbles about the size of human alveoli (diameter of 100 $\mu$m). The high mechanical stability as well as the absence of substantial film flow, inherent to small air bubbles, allowed for scanning force microscopy (SFM) directly at the air-water interface. The SFM topographical structure was correlated to the local distribution of fluorescent-labeled dipalmitoylphosphatidylcholine, as revealed from fluorescence light microscopy of the same bubbles. Although SFM has proven before to be exceptionally well suited to probe the structure of molecular films of pulmonary surfactant, the films so far had to be transferred onto a solid support from the air-water interface of a film balance, where they had been formed. This made them prone to artifacts imposed by the transfer. Moreover, the supported monolayers disallowed the direct observation of the structural dynamics associated with expansion and compression of the films as upon breathing. The current findings are compared in this respect to our earlier findings from films, transferred onto a solid support.

## INTRODUCTION

There is a class of surface-active, amphiphilic substances that form insoluble molecular films on water. They exhibit a water-soluble polar or charged region immersed in the water and a highly apolar region exposed toward the air. The insight gained of the physical and chemical properties of these substances is of great theoretical and practical importance in areas ranging from polymer science and nonlinear optics to biophysics. They also occur naturally as mixed phospholipid-protein layers covering epithelia. Pulmonary surfactant (PS) is the most prominent and medically important example. It forms a molecular film at the interface of the respiratory gas lumen to the solvation layer that covers the alveolar epithelium of vertebrate lungs. The film pressure counteracts the surface tension of the air-water interface. The work of breathing is thus strongly reduced and stability provided to the alveoli of different sizes (Pattle, 1955; Clements, 1957). The most abundant molecular species of PS, dipalmitoylphosphatidylcholine (DPPC), is also its most potent surface-tension-reducing agent (Watkins, 1968). However, unlike any pure phospholipid film, PS keeps the surface tension low over the large area excursions experienced in the lung during breathing (up to 30%). The underlying molecular mechanisms that also involve at least two of the surfactant-associated proteins (SP-C and SP-B) are a matter of investigation in the context of defunct surfactant in prematurely born children (infantile respiratory distress syndrome) and adults (Robertson and Halliday, 1998).

To probe their function, samples of PS may be prepared at the air-water interface of a film balance (i.e., a Langmuir balance) or of an air bubble (Enhorning, 1977; Schürch et al., 1989), where they can be compressed and the surface tension measured at the same time as a function of the mean interfacial area per molecule. The film architecture may be investigated by various spectroscopic and microscopic techniques (Ulman, 1991). Among the latter, scanning force microscopy (SFM) allows resolving the topography at the molecular level, and fluorescence light microscopy (FLM) shows the lateral distribution of particular components or reveals the pattern of some component in different physical states (Lee et al., 1998). By using SFM in conjunction with FLM we developed a molecular picture of the structure-function relationship of a PS model system containing SP-C (von Nahmen et al., 1997; Amrein et al., 1997; Kramer et al., 2000). The structures caused by SP-B or both types of surfactant proteins together were evaluated by Lipp et al. (1998) and Krol et al. (2000a,b). Recently, a spatially resolved chemical analysis by time-of-flight secondary ion mass spectrometry of the domain structures observed by fluorescence microscopy and the scanning techniques has been reported (Bourdos et al., 2000).

Up to now, SFM of PS and also the mass spectrometric analysis required the films to be transferred onto a solid support. Such a transfer may, however, perturb the molecular order resulting in a possible phase transition (Graf and Riegler, 1998). There may also be ambiguities as to the film's topology. To evaluate the earlier established models on supported monolayers, we now performed SFM directly

*Received for publication 29 December 2000 and in final form 10 September 2001.*

D. Knebel's present address: JPK Instruments AG, Bouchéstrasse 12, D-12435 Berlin, Germany.

Address reprint requests to Dr. M. Amrein, Universitatsklinikum Essen, Hufelandstrasse 55, 45122 Essen, Germany. Fax: 49-201-723-5911; E-mail: matthias.amrein@uni-essen.de.



0006-3495/02/01/474/07 $2.00

at the air-water interface of small air bubbles instead of a conventional film balance. Those air bubbles are mechanically stable, and they come very close to the alveoli with respect to their size and geometry.

## MATERIALS AND METHODS

### Air bubbles

Air bubbles of ~100 $\mu$m in diameter were produced in a buffer solution. They were anchored to hydrophobic areas on an otherwise hydrophilic mica support. The hydrophobic areas (size: 100 $\mu$m × 100 $\mu$m; eight patches per millimeter) were made by evaporating Cr (3 nm) and then Au (5 nm) onto freshly cleaved mica across a mask in a high-vacuum apparatus. The sample was then soaked for 30 min in 1 mM octanethiol (Fluka, Neu-Ulm, Germany) and rinsed extensively in ethanol (Merck, Darmstadt, Germany) and Milli-Q water (Milli-$Q_{185}$Plus, Millipore, Eschborn, Germany). This resulted in a hydrophobic, self-assembled monolayer of octanethiol, chemisorbed to the gold-covered areas, whereas the mica regions remained uncovered. Now, a drop of buffer containing 25 mM Hepes and 3 mM $CaCl_2$ (pH 7.0) was placed on the support. Subjecting the sample to reduced air pressure (20 kPa) in an airtight chamber resulted in the growth of bubbles adherent to the hydrophobic patches. The hydrophilic mica paths between the hydrophobic areas prevented the bubbles from spreading from hemispherical to a more flattened shape and kept the amphiphilic molecules from creeping from the air-water interface onto the support after an interfacial film had been adsorbed (see below). Once the bubbles had formed, the pressure was increased to ambient and most of the buffer replaced to prevent the bubbles from dissolving again.

### Film formation at the air-water interface

To obtain a molecular film of pulmonary surfactant at the air-water interface of the bubbles, small unilamellar vesicles were allowed to adsorb to the interface. We used a model surfactant system consisting of DPPC: DPPG (4:1 molar ratio), SP-C (0.4 mol %), and 2-(4,4-difluoro-5-methyl-4-bora-3a, 4a-diaza-*s*-indacene-3-dodecanoyl)-1-hexadecanoyl-*sn*-glycero-3-phosphocholine (BODIPY-PC) as a fluorescent dye (0.4 mol %). Vesicles of this system were prepared as described in Woodle and Papahadjopoulos (1989). 1,2-Dipalmitoyl-*sn*-glycero-3-phosphocholine (DPPC), 1,2-dipalmitoyl-*sn*-glycero-3-(phospho-*rac*-(1-glycerol)) (DPPG) were purchased from Avanti Polar Lipids (Alabaster, AL). BODIPY-PC was purchased from Molecular Probes (Eugene, OR). Recombinant dipalmitoylated SP-C was a generous gift from Byk-Gulden Pharmaceuticals (Konstanz, Germany) (Schilling et al., 1987). The vesicles were added to the sample to a final phospholipid concentration of 0.02 mM and the buffer stirred. The vesicles were allowed to adsorb for 5 min.

### Microscopy

The bubbles were observed in a fluorescent light microscope before a scanning force microscope. For the FLM, an immersion objective (63×, NA 1.32) and a pinhole size of 2.5 optical units were used in a commercial laser scanning confocal FLM (TCS 4D Leica, Heidelberg, Germany), BODIPY-PC fluorescence was excited with the 488-nm line of an air-cooled Ar-Kr laser, and emission was measured beyond 510 nm. Data acquisition was with eight-fold frame averaging.

For SFM, the sample was installed in the fluid cell of the microscope. The tip now could easily approach the interface of the air bubbles from above (Fig. 1). A soft cantilever (OMCL-TR400PS spring constant: 90mN/m, Olympus, Tokyo, Japan) and a homebuilt fluid cell were used together with a commercial SFM (Autoprobe CA, Park Scientific Instruments, Sunnyvale, CA).

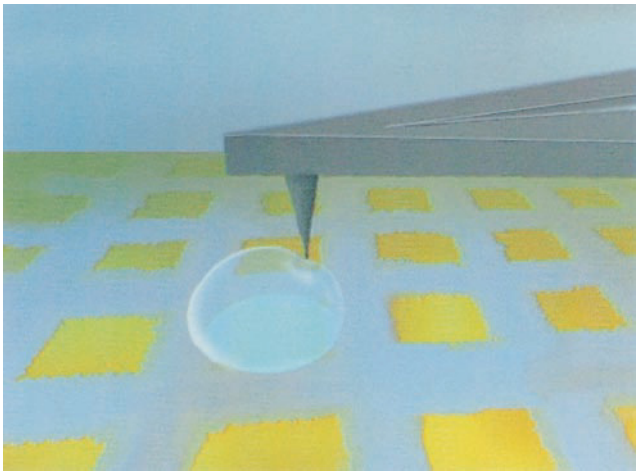

FIGURE 1 Illustration of the air bubble underneath the SFM probe (not to scale). The bubble is anchored to the support by a hydrophobic patch. The bubble was grown by subjecting the sample to reduced air pressure.

## RESULTS

Fig. 2 shows a data set of the top part of a bubble upon the adsorption of the model surfactant system, acquired by a confocal FLM. At the interface, a phase-separated film with dark domains embedded in a bright background took shape.

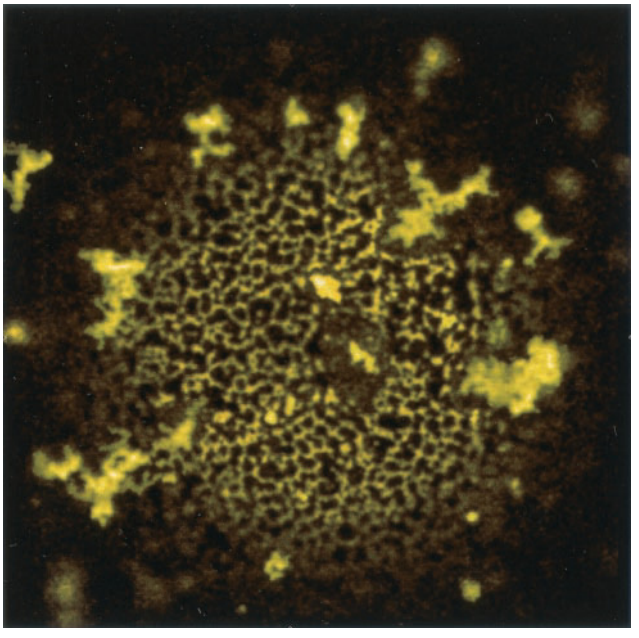

FIGURE 2 Data set from a laser scanning confocal FLM (TCS 4D, Leica, Heidelberg, Germany) of the top part of a bubble upon the adsorption of the model surfactant system; 200 $\mu$m × 200 $\mu$m). It has been shown earlier that the dye is always found in the same phase as the SP-C (von Nahmen et al., 1997). Hence, there are polygonal lipid patches that are surrounded by a protein-rich rim. In addition to the film at the air-water interface, there are large clusters of vesicular matter that are tightly anchored to the bubble surface. Apparently, the film formed from these extended clusters.

We showed earlier that in these films the bright areas contain the peptide SP-C in addition to the fluorescent dye and some of the lipid, whereas the dark areas are a condensed phase of a protein-depleted but DPPC-enriched monolayer (von Nahmen et al., 1997; Galla et al., 1998; Bourdos et al., 2001). The film in Fig. 2 was fully at rest within the resolution of the light microscope. This indicated that the film had reached its equilibrium surface pressure of ~50 mN/m (resulting in a surface tension of 23 mN/m) and, hence, a highly condensed state (Post et al., 1995). Note that there are aggregates of vesicular matter tightly attached to the interface. Both the formation of an interfacial film as well as the aggregation of vesicles were dependent on the presence of $Ca^{2+}$ in the buffer.

To be able to perform SFM at the bubble's interface, all excessive vesicles and their large aggregates had to be removed. This was accomplished by exchanging the buffer several times by a buffer devoid of $Ca^{2+}$ (25 mM Hepes, 0.1 mM EDTA, pH 7,0). EDTA was added to chelate any remaining $Ca^{2+}$. It is noteworthy that the film at the interface was not disturbed by the removal of the $Ca^{2+}$ from the buffer as revealed by FLM.

Fig. 3 shows the appearance of the bubble in the SFM. The SFM raw data (Fig. 3 *A*) expose the overall shape of the bubble. When the image is flattened computationally, the film topology becomes apparent (Fig. 3 *B*). There are two topologically distinct areas with a height difference that varies between 4 and 5 nm (Fig. 3 *C*). This is close to the thickness of a fluid lipid bilayer of DPPC and/or DPPG (Rand and Parsegian, 1989). Hence, the lower area may correspond to a molecular monolayer at the air-water interface, whereas the elevated area appears to be a fluid lipid bilayer on top of the monolayer, as judged from its height. From comparison with an accompanying FLM image (Fig. 3 *D*), it is evident that the fluorescent areas correspond to the elevated regions in the topography, whereas the dark areas correspond to the lower regions. In some places, a small piece of a second bilayer appears on top of the first one (arrow in Fig. 3 *B*). Such different levels of thickness of the film become apparent also in the FLM. They appear as distinct levels of brightness (e.g., at the intersections of the netlike fluorescent phase in Fig. 2) if the multi-layered areas are not too small to be resolved by the light microscope.

## DISCUSSION

### Film structure

Multilamellar areas in equilibrium with monomolecular regions are a general feature of pulmonary surfactant films. They have been observed in vivo at the air-saline interface of alveoli by electron microscopy of thin sections of rabbit lungs (fixed by vascular perfusion) (Schürch et al., 1995). Amrein et al. (1997) showed that the relative amount of material within these domains depends on the surface pressure that has been applied. The multi-layered structures formed only if the film was compressed beyond the molecular area, where its equilibrium surface pressure of 50 mN/m was reached. The current study now shows that the multilamellar structures also form spontaneously (i.e., without the need of film compression) when the surfactant matter is spread from vesicles to the interface.

The multi-layered areas in equilibrium with the remaining monolayer are thought to play an important role in the functional pulmonary surfactant. This matter apparently acts as a reservoir of surface-active material that immediately replenishes the molecular film, once the lung's interface is increased upon breathing. As a consequence, the film remains in a condensed state, and the surface tension does not rise above the equilibrium value. The reservoir forms by two distinctive mechanisms: it spontaneously builds up upon the adsorption of surfactant material to the interface, and it forms upon compression of the film. The SP-C is thought to be responsible for this function because lamellae do not form reversibly in pure lipid films. The peptide's highly hydrophobic $\alpha$-helical part is thought to span the lipid bilayers and thereby acts as a molecular lever that moves the lipids back and forth between the monolayer and the lamellar phase.

The present SFM study performed directly at the air-water interface proved to be of advantage in several aspects compared with studies of films transferred onto a solid support. In the latter case, it could not be determined whether the multi-layer phase had formed toward the air or the former aqueous sub-phase (Fig. 4). They were now found to be oriented at least in part toward the aqueous phase. Furthermore, after the transfer, the lipid bilayers were always found to be substantially thicker than in the current study (>6 nm as compared with 4–5 nm). They might therefore have been in a more condensed state, as judged from their thickness, as a result of the transfer. It is notable that SP-C is more likely to reside in a lipid bilayer in the fluid phase as compared with a bilayer in the gel phase (Johansson and Curstedt, 1997).

### SFM imaging at the air-water interface

To shed light on the imaging process itself, also bubbles without a film at the air-water interface were evaluated. Fig. 5 *A* shows an SFM topography of the apex of an air bubble in Milli-Q water without any film. For imaging, the SFM tip was loaded with ~1 nN onto the bubble's interface. It is an obvious prerequisite for successful imaging that the bubble must counteract the load of the tip. The force-sample position curve (Fig. 5 *B*) allows evaluation of this interaction. When the air-water interface approaches the tip, there is an attractive force bringing about a snap-on between the tip and the air bubble. Once the tip is in contact with the air-water interface, the surface tension $\gamma$ starts to counteract the deformation of the bubble by the tip. This is because the

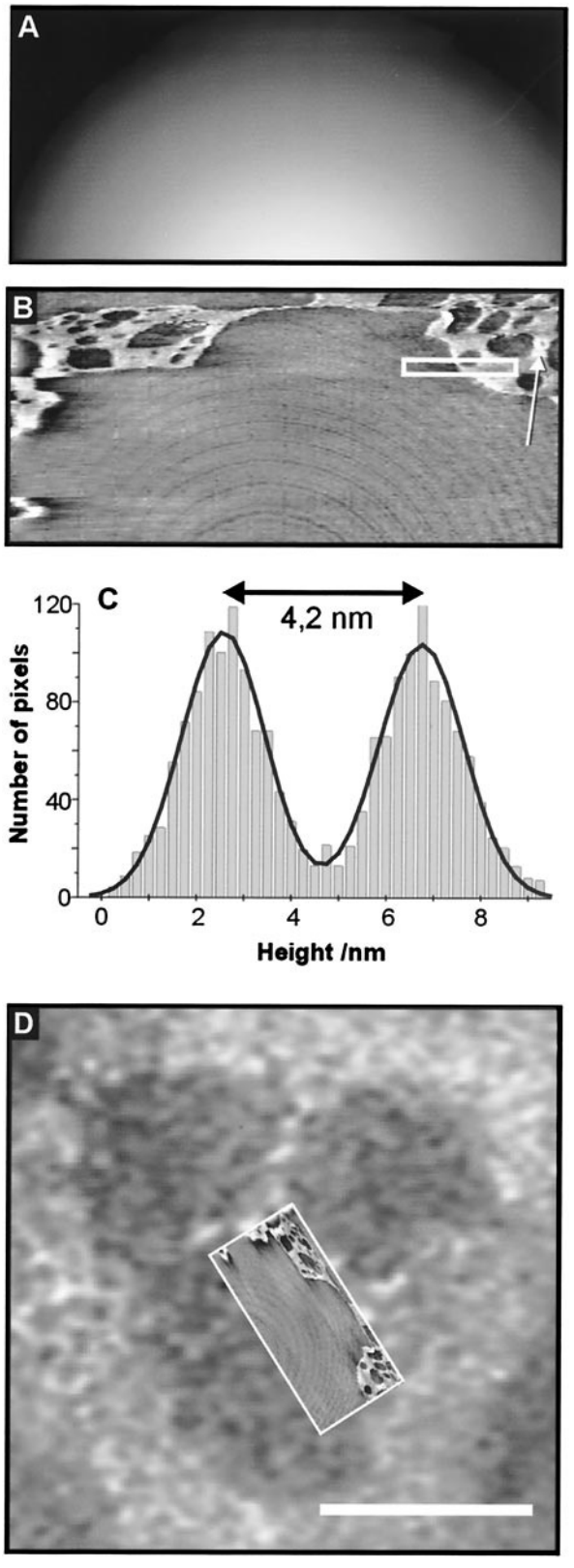


FIGURE 3 (*A*) SFM topography of an air bubble, covered by a molecular film of the surfactant model system (25 $\mu$m $\times$ 12 $\mu$m; gray scale: 2 $\mu$m). (*B*) After subtraction of the nearly spherical shape of the bubble (gray scale: 10 nm), there are two distinct levels of height with the elevated region ~4–5 nm above the lower area. The concentric rings visible in the lower area are centered in the apex of the bubble. They are most probably due to the capillary waves. (*C*) The histogram of the boxed area in *B* reveals a height of 4.2 nm of the elevated area. This is closer to the value of a bilayer of DPPC or DPPG in the liquid phase than in the gel phase (Rand and Parsegian, 1989). (*D*) FLM micrograph of the bubble (bar, 25 $\mu$m). The SFM topography is inset at a likely position. Note that the fluorescent areas correlate with the elevated regions (i.e., the double-layer structures contain the fluorescent dye).

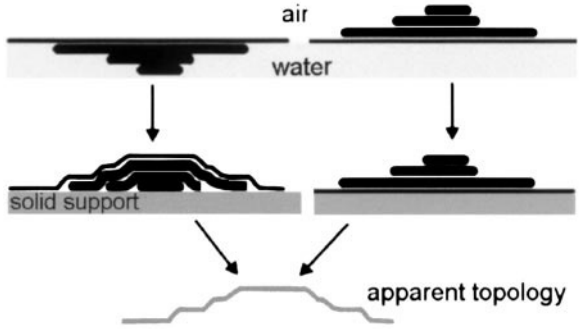


FIGURE 4 Illustration of one of the ambiguities inherent to SFM topographies, if the films are transferred from the air-water interface to a solid support before the microscopy.

surface area of the bubble increases when it becomes deformed and brings about the following energy difference:

$$\Delta E = \gamma \Delta A \tag{1}$$

With the simple assumption of the interface nestled against a hydrophilic tip with a spherical apex (Fig. 6 *A*, left), the force $F$ is calculated as:

$$F = 2\pi\gamma t, \tag{2}$$

where $t$ is the penetration depth of the tip with respect to the undisturbed air-water interface. Equation 2 explains the observed linearity of the force-sample position curve (Fig. 5 *B*) after the tip has started to indent the bubble, but the slope calculates to be higher than is experimentally observed (i.e., the bubble is less stiff in the experiment than expected from Eq. 2). This is because the interface will adopt a surface shape of lower energy than the simple geometry assumed for Eq. 2 (Fig. 6 *A*, right). Interestingly, when the interface of the bubble, coated with pulmonary surfactant, was approached to the tip, it resisted its deformation about as strongly as the bubble without a molecular film, as judged from a similar slope of the force-sample position curve (not shown). On the other hand, it follows from Eq. 2 that the surface tension now must have contributed much less to the stiffness of the bubble because of its lower value (~20 mN/m in the case of the surfactant-coated interface as compared with ~70 mN/m for the free interface). However, the molecular film by itself may now have contributed to the stiffness of the bubble. Like a plate, it may have resisted

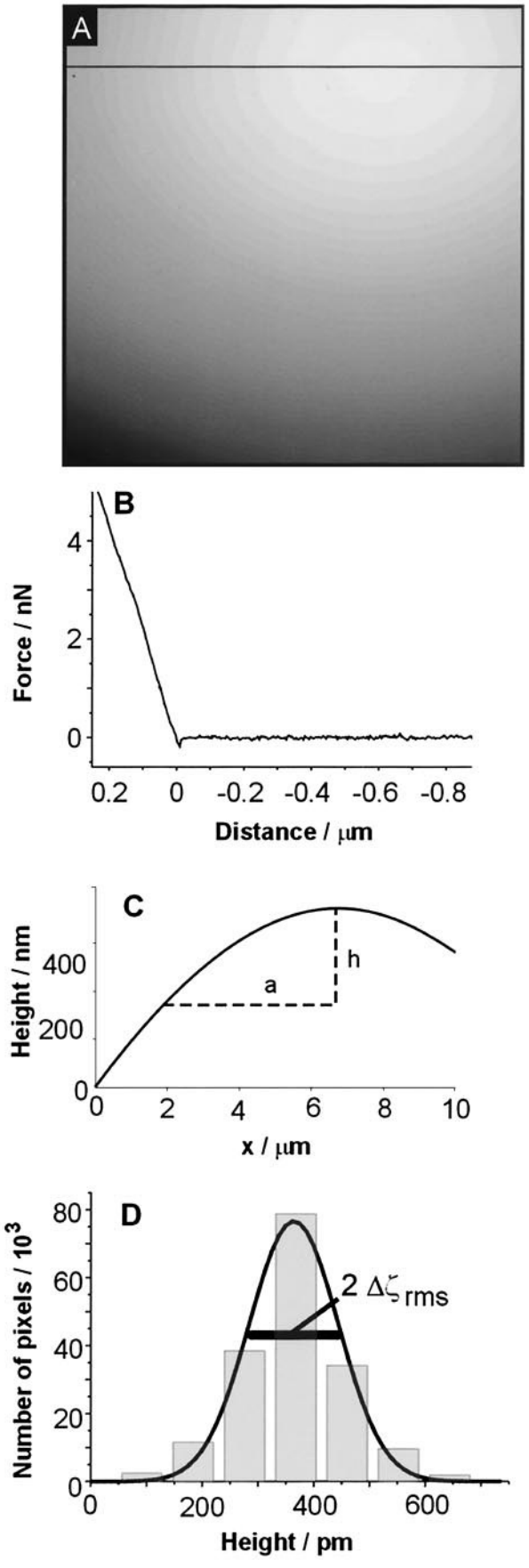


becoming bent, according to its bending (splay) elasticity $\kappa$ (Fig. 6 *B*) (Helfrich, 1975). To bend the film around the tip (Fig. 6 *B*, left) results in a force:

$$F = 4\pi\kappa/R \tag{3}$$

Unfortunately, no values for $\kappa$ are published for monomolecular lipid layers. However, for fluid double layers of phospholipids the documented values range from $2E - 19$ J and $0.24E - 19$ J (Niggemann et al., 1995). Assuming $\kappa = 2E - 19$ J and $R = 5$ nm, the force calculates to be 0.5 nN. Again, this is only a rough estimate. The curvature adopted by the bubble will certainly differ from the assumed geometry in that there will be a steady transition to the undisturbed air-water interface similar to the case without any film (Fig. 6 *B*, right).

Another important concern for SFM imaging is the possibility of the bubble being vibrating. There are two possible vibration modes of the bubble that might disturb SFM imaging: the oscillation of the volume and the capillary waves. The eigenfrequency of the former can be calculated as (Devin, 1959)

$$f_V = 1/2\pi r\sqrt{3\vartheta p/\rho}, \tag{4}$$

where $r$ is the radius of the air bubble, $\vartheta = c_P/c_V$ is the quotient of the specific heats of the air, $p$ is the surrounding pressure, and $\rho$ is the density of the liquid. The first eigenfrequency of the capillary waves is (Lamb, 1924)

$$f_K = 1/2\pi r\sqrt{12\gamma/\rho r}, \tag{5}$$

where $\gamma$ is the surface tension. For example, $f_V = 65$ kHz and $f_K = 7$ kHz with $\gamma = 20$ mN/m and $r = 50$ $\mu$m. These frequencies lay above the typical frequencies occurring in the data stream of the SFM. Therefore, they are not expected to disturb the imaging. On the other hand, some standing waves of the oscillation may become apparent in the SFM topography (Fig. 3).

Mechanical noise is another important concern when imaging an air bubble. It may be evaluated from the apparent corrugation of the air-water interface of an uncoated bubble as shown in Fig. 5, because the interface should be devoid of any real structure accessible to the SFM. Fig. 5 *D*

FIGURE 5 (*A*) SFM topography of an air bubble in ultra-pure water without any interfacial film. The picture is 10 $\mu$m $\times$ 10 $\mu$m, the height range (gray scale) is 400 nm. (*B*) Force-sample position curve. The tip is approached to the interface from the right to the left, and the force is calculated from the deflection of the cantilever. Apparently, the bubble behaves to a first approximation as a harmonic spring, as judged from the linear increase of force after contact is made. (*C*) From the line scan across the apex of the bubble (black line in *A*) the diameter of the air bubble calculates as $(a^2 + h^2)/h = 112$ $\mu$m. (*D*) Histogram of the apparent surface roughness of the bubble. Because the naked air-water interface is expected to be perfectly smooth, the surface roughness reveals the noise inherent in the image.

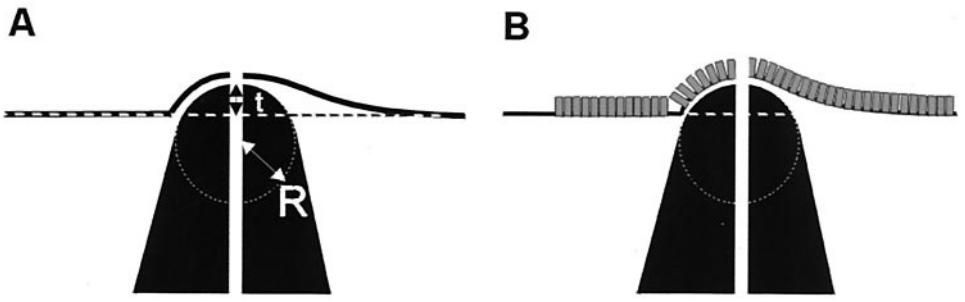


FIGURE 6 Deformation of the bubble by the SFM tip, without any film (*A*) and with a molecular film at the interface (*B*). The left part of each figure depicts the interface nestling against the tip. This simplified geometry has been assumed to estimate the tip-sample interaction. On the right of *A* and *B*, respectively, more likely situations are sketched.

represents a histogram of the height distribution of the bubble due to noise (after subtraction of the overall bubble shape). Apparently, the noise does not substantially disturb the imaging as it results in an apparent corrugation of only ~80 pm (Fig. 5 *D*). Note that this does not necessarily translate into an accordingly high structural resolution in the case of a molecular film at the interface. This is because the structural resolution is a function of more parameters, such as the actual tip geometry.

SFM directly at the air-water interface opens the perspective to vary the size of the bubble and, hence, the state of compression, to study in situ the molecular rearrangements associated with this process. Interestingly, SFM in principal not only allows deducing the molecular architecture of the interfacial film, but it may also be used to determine the surface tension $\gamma$ of the interface. The rule of Laplace reveals as a function of $\gamma$ the pressure difference across an interface (Landau and Lifschitz, 1991):

$$\Delta p = \gamma(c_1 + c_2), \tag{6}$$

with $c_1$ and $c_2$ being the main curvatures of the interface as they may directly be taken from the SFM image. Because the pressure difference across the interface is not known, the rule of Laplace may be combined with an expression describing the deformation of the clinging bubble from spherical due to the hydrostatic pressure (Andreas et al., 1938). Up to now there is no analytical solution for $\gamma$ from the combined expression, but a fast numerical approach is available (Skinner et al., 1989). Note that for the determination of $\gamma$, the SFM images need to be accurately corrected for image distortions due to thermal drift and hysteresis of the piezo-ceramic scanning elements. Furthermore, the contact line between the bubble and the support needs to be perfectly circular. Both conditions have not yet been fully met in the current study.

### Future perspectives

Pulmonary surfactant contains at least three more specific proteins (SP-A, SP-B, and SP-D) in addition to SP-C and many additional lipid species that were not used in the current study. Much of their role in film formation and surface activity is still highly speculative and might be approached by using the technique described in this report. Once the SFM at the air-water interface is now established, scanning near-field optical microscopy and additional scanning probe techniques may be applied as well. Furthermore, force-distance curves might elucidate how particles such as silicon dust interact with the surfactant (Butt, 1994), an issue of considerable medical significance. The method might also prove highly valuable for the investigation of surface-active substances other than pulmonary surfactant.

We acknowledge L. Melanson for careful corrections, Dr. U. Kubitschek for his collaboration to obtain Fig. 3, and M. Messerli, CEO Bitplane AG, Zürich, for data processing of Fig. 3. We further thank Dr. A. G. Bitterman for drawing Fig. 1.

This work was supported by the IMF (Innovative Medizinische Forschung) at the University of Münster, Germany (grants RE-1–5-II/96–16 and RE-1–5-II/97–26) and the DFG (grants Si 670 and AM III/3–1).

## REFERENCES

Amrein, M., A. von Nahmen, and M. Sieber. 1997. A scanning force- and fluorescence light microscopy study of the structure and function of a model pulmonary surfactant. *Eur. Biophys. J.* 26:349–357.

Andreas, J. M., E. A. Hauser, and W. B. Tucker. 1938. Boundary tension by pendant drops. *J. Phys. Chem.* 42:1001–1019.

Bourdos, N., F. Kollmer, A. Benninghoven, M. Ross, M. Sieber, and H. J. Galla. 2000. Analysis of lung surfactant model systems with time-of-flight secondary ion mass spectrometry (TOF-SIMS). *Biophys. J.* 79: 357–369.

Butt, H.-J. 1994. A technique for measuring the force between a colloidal particle in water and a bubble. *J. Colloid Interface Sci.* 166:109–117.

Clements, J. A. 1957. Surface tension of lung extracts. *Proc. Soc. Exp. Biol. Med.* 95:170–172.

Devin, C. J. 1959. Survey of thermal, radiation, and viscous damping of pulsating air bubbles in water. *J. Acoust. Soc. Am.* 31:1654–1667.

Enhorning, G. 1977. A pulsating bubble technique for evaluating pulmonary surfactant. *J. Appl. Physiol.* 43:198–203.

Galla, H. J., N. Bourdos, A. von Nahmen, M. Amrein, and M. Sieber. 1998. The role of pulmonary surfactant protein C during the breathing cycle *Thin Solid Films.* 327:632–635.

Graf, K., and H. Riegler. 1998. Molecular adhesion interactions between Langmuir monolayers and solid substrates. *Colloids Surfaces A Physicochem. Eng. Aspects.* 131:215–224.

Helfrich, W. 1975. Out-of-plane fluctuations of lipid bilayers. *Z. Naturforsch. C.* 30:841–842.

Johansson, J., and T. Curstedt. 1997. Molecular structures and interactions of pulmonary surfactant components. *Eur. J. Biochem.* 244:675–693.

Kramer, A., A. Wintergalen, M. Sieber, H.-J. Galla, M. Amrein, and R. Guckenberger. 2000. Distribution of the surfactant-associated protein C within a lung surfactant model film investigated by near-field optical microscopy. *Biophys. J.* 78:458–465.

Krol, S., A. Janshoff, M. Ross, and H-J. Galla. 2000a. Structure and function of surfactant protein B and C in lipid monolayers: a scanning force microscopy study. *Phys. Chem. Chem. Phys.* 2:4586–4593.

Krol, S., M. Ross, M. Sieber, S. Künneke, H.-J. Galla, and A. Janshoff. 2000b. Formation of three-dimensional protein-lipid-aggregates in monolayer films induced by surfactant protein B. *Biophys. J.* 79: 904–918.

Lamb, H. 1924. Hydrodynamics. Cambridge University Press, Cambridge, UK.

Landau, L. D., and E. M. Lifschitz. 1991. Hydrodynamik. Akademie Verlag, Berlin.

Lee, K. Y. C., M. M. Lipp, D. Y. Takamoto, J. A. Zasadzinski, and A. J. Waring. 1998. Direct observation of phase and morphology changes induced by lung surfactant protein SP-B in lipid monolayers via fluorescence, polarized fluorescence, and atomic force microscopies. *SPIE Proc.* 3273:115–133.

Lipp, M. M., K. Y. C. Lee, D. Y. Takamoto, J. A. Zasadzinski, and A. J. Waring. 1998. Coexistence of buckled and flat monolayers. *Phys. Rev. Lett.* 81:1650–1653.

Niggemann, G., M. Kummrow, and W. Helfrich. 1995. The bending rigidity of phosphatidylcholine bilayers: dependence on experimental method, sample cell sealing and temperature. *J. Phys. II France.* 5:413–425.

Pattle, R. E. 1955. Properties, function and origin of the alveolar lining layer. *Nature.* 175:1125–1126.

Post, A., A. V. Nahmen, M. Schmitt, J. Ruths, H. Riegler, M. Sieber, and H. J. Galla. 1995. Pulmonary surfactant protein C containing lipid films at the air-water interface as a model for the surface of lung alveoli. *Mol. Membr. Biol.* 12:93–100.

Rand, R. P., and V. A. Parsegian. 1989. Hydration forces between phospholipid bilayers. *Biochim. Biophys. Acta.* 988:351–376.

Robertson, B., and H. L. Halliday. 1998. Principles of surfactant replacement. *Biochim. Biophys. Acta.* 1408:346–361.

Schilling, J. W. Jr., R. T. White, and B. Cordell. 1987. Recombinant alveolar surfactant protein. US Patent 4.659,805.

Schürch, S., H. Bachofen, J. Goerke, and F. Possmayer. 1989. A captive bubble method reproduces the in situ behavior of lung surfactant monolayers. *J. Appl. Physiol.* 67:2389–2396.

Schürch, S., R. Qanbar, H. Bachofen, and F. Possmayer. 1995. The surface-associated surfactant reservoir in the alveolar lining. *Biol. Neonate.* 1:61–76.

Skinner, F. K., Y. Rotenberg, and A. W. Neumann. 1989. Contact angle measurements from the contact diameter of sessile drops by means of a modified axisymmetric drop shape analysis. *J. Colloid Interface Sci.* 130:25–34.

Ulman, A. 1991. An Introduction to Ultrathin Organic Films. Academic Press, Boston.

von Nahmen, A., A. Post, H. J. Galla, and M. Sieber. 1997. The phase behavior of lipid monolayers containing pulmonary surfactant protein C studied by fluorescence light microscopy. *Eur. Biophys. J.* 26:359–369.

Watkins, J. C. 1968. The surface properties of pure phospholipids in relation to those of lung extracts. *Biochim. Biophys. Acta.* 152:293–306.

Woodle, M. C., and D. Papahadjopoulos. 1989. Liposome preparation and size characterization. *Methods Enzymol.* 171:193–217.